Proceedings of 3rd International Civil Engineering and Architecture Congress (ICEARC'23)
DOI 10.31462/icearc.2023.sme137

The frictional and elastomeric seismic joint apparatus and its usage as a steel beam-to-column connection

Orkun Yılmaz[1*], Serkan Bekiroğlu[1]

[1] Yildiz Technical University, Faculty of Civil Engineering, Department of Civil Engineering, İstanbul, Türkiye

Abstract

Purpose: This study presents a new fuse connection, which is a replaceable seismic joint apparatus that ensures that no structural member is damaged, including itself.
Study design/methodology/approach: Three beam-to-column connections, one of which is formed with the frictional and elastomeric joint apparatus, one of which is formed with the four-bolted unstiffened end-plate, the other is formed with the four-bolted stiffened end-plate, were analyzed via non-linear finite element simulation. HE240A beam and HE300B column were used in the connections. All the connections were analyzed under cyclic loading until the end of the 7% radian story drift angle.
Findings: The finite element analyses show that the beam-to-column connection with the frictional and elastomeric seismic joint apparatus has more energy dissipation capacity and can transfer more moment value compared with the bolted end-plate connections. Moreover, the beam-to-column connection with the frictional and elastomeric seismic joint apparatus has displayed no damage in any structural member, including itself. However, the bolted end-plate connections have displayed local buckling failure on the beam.
Originality/value: The frictional and elastomeric seismic joint apparatus is at a level that can compete with its foreign patented counterparts, thanks to its replaceability, as well as having the desired strength and flexibility of the moment connection types presented in Türkiye Building Earthquake Regulation-2018. In addition, the patent processes are currently progressing in the presence of TÜRKPATENT, the United States Patent and Trademark Office, and the European Patent Office.

Keywords: Replaceable Connection; Seismic Joint Apparatus; Fuse Connection; Beam-To-Column Connection; Finite Element Simulation.

1. Introduction

Steel moment frame systems are widely used due to their high ductility capacity. According to the Türkiye Building Earthquake Regulation (TBER-2018), moment beam-to-column connections should be proven to satisfy at least a 4% radian story drift angle. In the TBER-2018, six beam-to-column connections that have been proven to be prequalified according to AISC 358-16 (AISC, 2020) are presented. The prequalified connections are designed to fail within the beam during a possible earthquake. In this approach, the structural framework of a building is allowed to develop limited failure due to the earthquake. The other approach is to use the fuse joint so that some components in joints of the structural framework are allowed to be damaged in the controlled damage zone, and the components can be replaced after an earthquake. Many researchers have been studied about the fuse joint systems to prevent the failure of structural members (Oh et al., 2009; Sarkisian et al., 2011; Shen et al., 2011; Calado et al., 2013; Tong et al., 2016; Sadeghi et al., 2017; Garoosi et al., 2018; Jiang et al., 2019; Richards, 2019; Francavilla et al., 2020; Yan et al., 2020; Peng et al., 2020;

* Corresponding author (yilmazo@yildiz.edu.tr)
© 2023 Authors. Publishing services by golden light publishing®.
This is an open-access article under the CC BY-NC-ND license (http://creativecommons.org/licenses/by-nc-nd/4.0/).

Molavi et al., 2020; Saravanan et al., 2021). Some of the developed fuse joint systems in the literature are shown in Fig. 1.

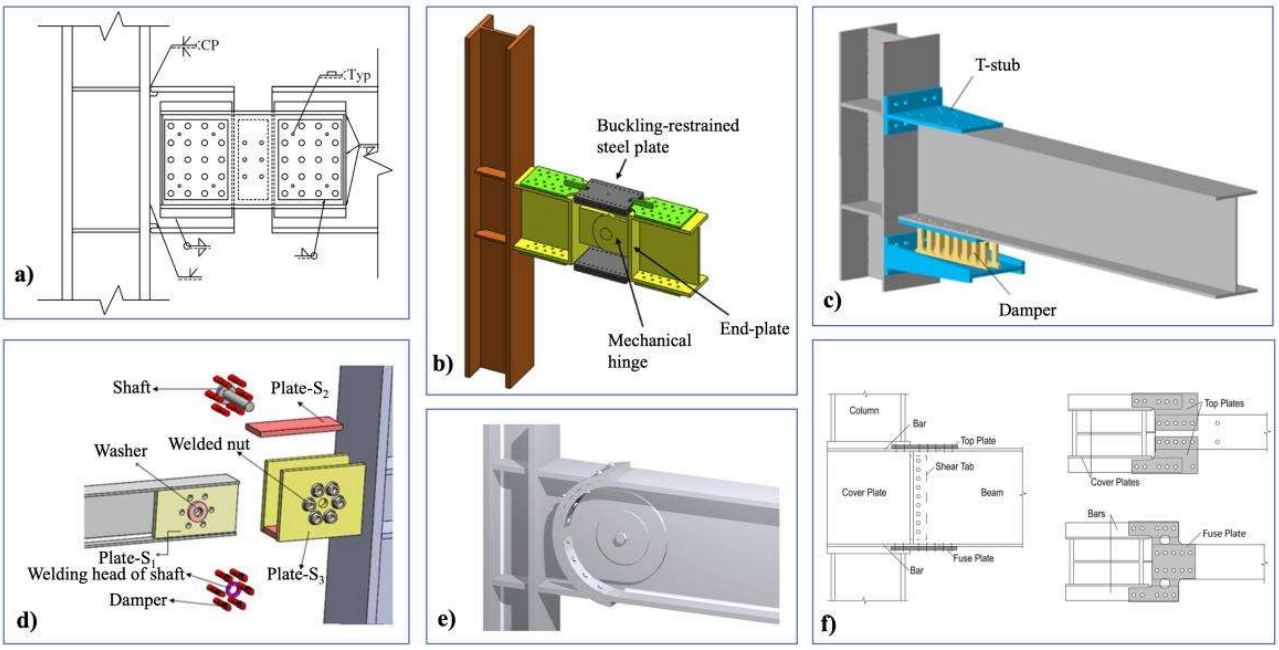


Fig. 1. Some of the developed fuse joint systems in the literature: **a)** Shen et al., 2011, **b)** Peng et al., 2020, **c)** Oh et al., 2009, **d)** Molavi et al., 2020, **e)** Sarkisian et al., 2011, **f)** Richards, 2019

The primary disadvantage of fuse joint is to replace the damaged apparatus. That is why innovation in the relevant technical field may be required. The present study introduces a new joint apparatus to eliminate the mentioned disadvantage and bring new advantages to the relevant technical field, especially when used in buildings. The main advantage of the developed apparatus is that replacement of the apparatus is not required, as the structural members, including the apparatus, remain essentially elastic. The apparatus can be applied in the connection of the structural members, such as steel beam-to-column connections and link members of the eccentrically braced frames. Moreover, the apparatus can be used to retrofit old reinforced concrete or steel buildings. For this study, only the usage of the apparatus as a beam-to-column connection example is presented. Ansys Workbench 2020 R2 (Ansys Inc., 2020), a finite element analysis software, was used for analyses in this study.

2. The proposed seismic joint apparatus

2.1. Configuration of the simple form

The simple configuration of the frictional and elastomeric seismic joint apparatus is seen in Fig. 2. The simple form of the joint apparatus consists of two outer plates, at least an inner plate, friction members, elastomers, master pin, additional bolts, and stiffness members. The friction members are welded to the outer plates so that a friction force occurs between the friction member and the inner plate. Additionally, the elastomers are glued to the outer and inner plates. The working principle of this apparatus and detailed information about it have been presented in previous studies (Yılmaz and Bekiroğlu, 2021; Yılmaz, 2022). Moreover, these studies demonstrated that the moment capacity of the friction members, elastomers, and apparatus can be obtained by Eqs. 1, 2, and 3, respectively.

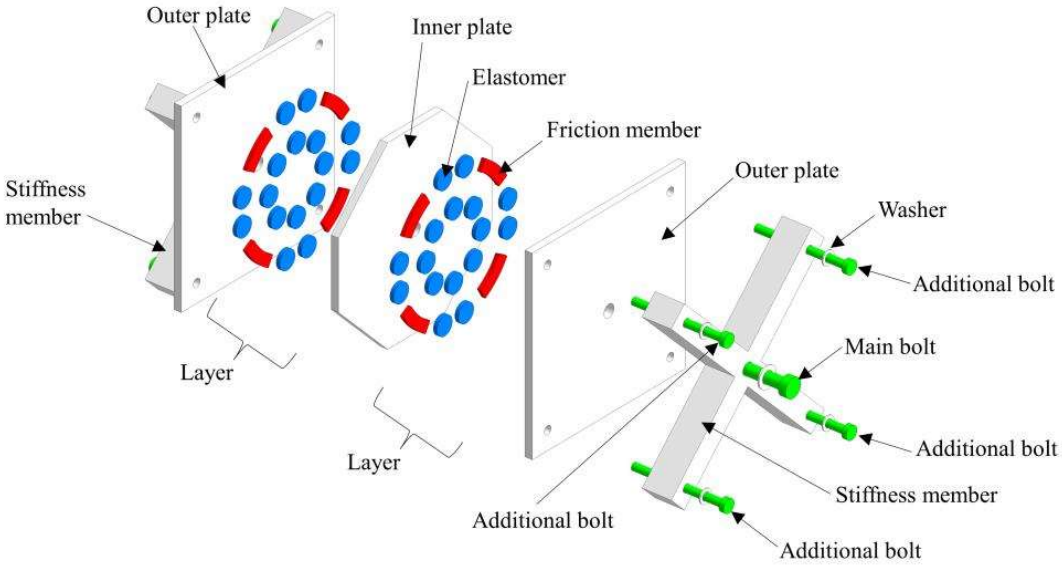


Fig. 2. The exploded 3D view and components of the simple form of the apparatus

$$M_F = T_F \cdot \mu \cdot x_F \tag{1}$$

$$M_E = \sum_{i=1}^{m} M_{E,i} = \sum_{i=1}^{m} \left(k_E \cdot y_{E,i} \cdot x_{E,i} \right) = \sum_{i=1}^{m} \left(k_E \cdot \theta \cdot x_{E,i}^2 \right) \tag{2}$$

$$M = n \cdot \left(T_F \cdot \mu \cdot x_F + \sum_{i=1}^{m} \left(k_E \cdot \theta \cdot x_{E,i}^2 \right) \right) \tag{3}$$

2.2. Application in a steel beam-to-column connection

The apparatus can be implemented in a beam-to-column connection in the steel frames. Although the design strategy is based on the remaining elastic of the structural members and the apparatus, the apparatus may need to be replaced for some reason, such as wear on the friction surfaces. The apparatus is connected to the column at point "C" as shown in Fig. 3(a). The center of the apparatus, in other words, the rotation point of the connection, is illustrated as point "A" and the apparatus is connected to the beam at point "B". As seen in Fig. 3(a), the moment capacity of the apparatus (M_{app}) is determined for the case that the beam-end section reaches the elastic moment capacity of the beam section (M_y). Hence, the moment capacity of the apparatus can be obtained using Eq. 4. As seen in Fig. 3(b), the initial rotational stiffness of the connection is not obtained infinite because before the friction members reach their friction capacity, the beam, column and apparatus exhibit bending behavior due to their elastic stiffness. The initial rotational stiffness of the connection (R_{in}) can be obtained from Eq. 5. Thus, the initial rotation value (θ_{in}) at which the sliding of the friction members begins can be calculated from Eq. 6.

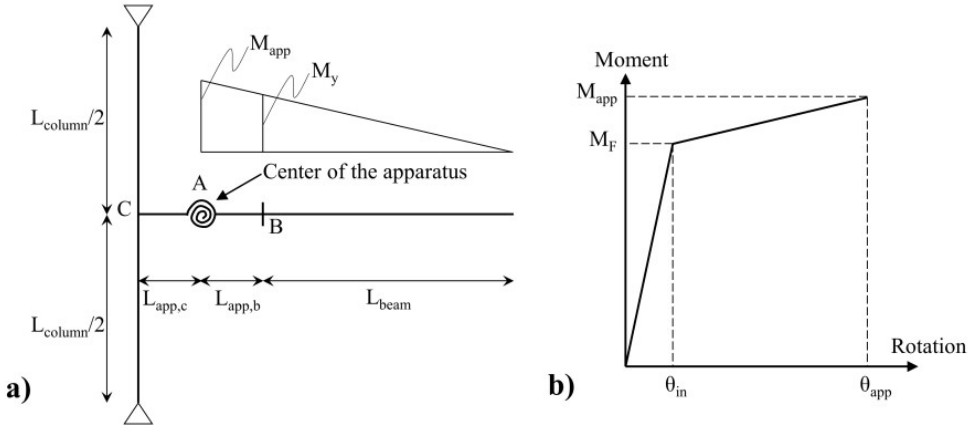


Fig. 3. Location of the apparatus and typical moment-rotation curve of the beam-to-column connection

$$M_{app} = M_y \left(L_{beam} + L_{app,b} \right) \Big/ L_{beam} \tag{4}$$

$$R_{in} = \frac{1}{\frac{1}{k_{beam}} + \frac{1}{k_{app,b}} + \frac{1}{k_{app,c}} + \frac{1}{k_{column}}} \tag{5}$$

$$\theta_{in} = \frac{M_F}{R_{in}} \tag{6}$$

The montage procedure of the frictional and elastomeric seismic joint apparatus to the beam and column is shown in Fig. 4. In order to connect the apparatus properly, the apparatus is lowered from above of the beam to the connection zone and fixed to the montage plates, which have been welded to beam and column, with the montage bolts. As seen in Fig. 4, the outer and inner plates have been extended, unlike the simple form shown in Fig. 2, so that the apparatus can be assembled with the montage bolts.

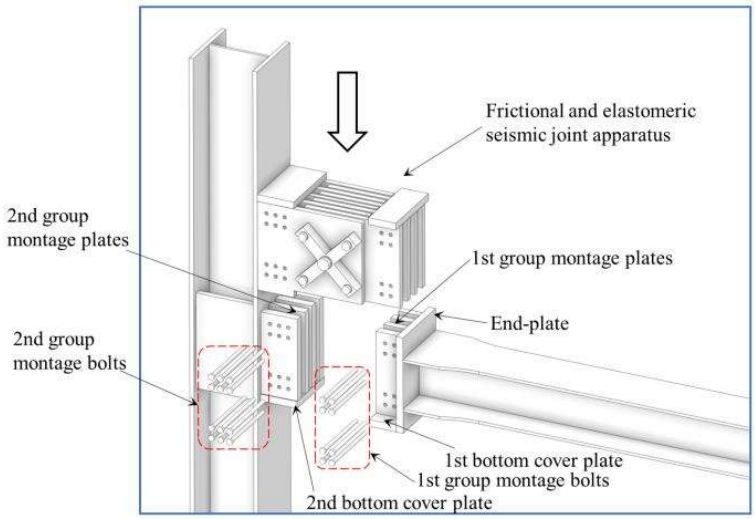


Fig. 4. The montage procedure of the apparatus to the beam and column

3. A numerical example and comparison with four bolted end-plate connections

3.1. Finite element models

A numerical example has been carried out to illustrate the application of the apparatus in a steel beam-to-column connection and the comparison of it with four bolted end-plate connections. For this reason, three beam-to-column connections, one of which is formed with the proposed seismic joint apparatus (FESA), one of which is formed with the four-bolt unstiffened end-plate (4E), the other is formed with the four-bolt stiffened end-plate (4ES), were designed and analyzed via non-linear finite element simulation. HE240A beam and HE300B column were used in the connections. ASTM A36 steel material was used for end-plate in 4E and 4ES connections and for end-plate stiffener in 4ES connection. ASTM A490 bolt material was used for all bolts, including main and additional bolts in FESA connection, in all connections. Moreover, neoprene rubber material with a shear modulus of G=0.723 MPa was used for elastomers in the FESA connection. For all components other than these, including beam and column, ASTM A572 grade 50 steel material was used in all connections. The material properties used in the finite element analyses can be seen in (Gerami et al., 2011; Yılmaz, 2022). The dimensions of the FESA connection are given in Fig. 5. If the design is made in such a way that the elastic moment capacity of the beam (M_y=232.19 kNm) occurs at the section where the beam is connected to the end-plate, M_{app} = 261.45 kNm is obtained by Eq. 4. The flanges of the beam section have been widened locally at the beam end to prevent plasticization due to possible stress and strain concentrations at the level of elastic moment value at the beam face as seen in Fig. 5.

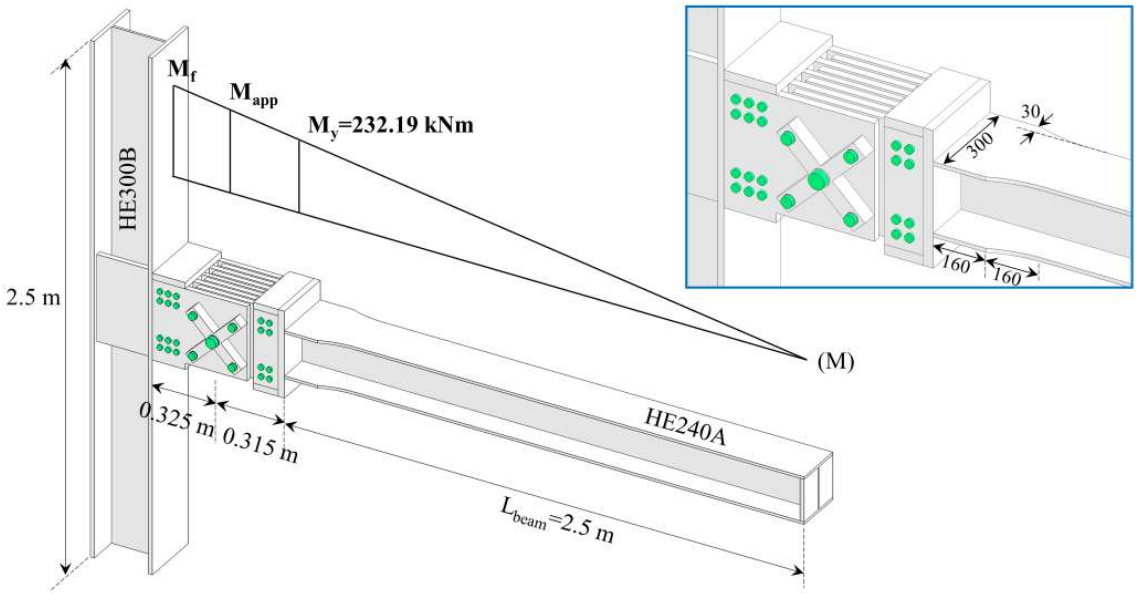


Fig. 5. The dimensions of FESA connection

The exploded 3D view of the apparatus used in the numerical example is given in Fig. 6. Eight layers (n=8) were considered due to the moment value to be transferred and the width of the beam flange. Moreover, the dimensions of the outer and inner plates are given in Fig. 7. The master pin, which consists of an M30 bolt with a 33 mm diameter bolt hole, is the rotation point of the connection. Four additional M20 bolts with a 22 mm diameter bolt hole have been used to ensure a more uniform compressive force on the apparatus. In addition, there are four slots on each inner plate so that the additional bolts can move freely when the apparatus rotates about the master pin. Bolt hole diameters on 1st and 2nd group montage plates and the outer and inner plates are 16 mm, as M16 tight fit pins have been used for 1st and 2nd group montage bolts. The geometric shape of the friction members was considered as the arc because it was seen that the stress distributions on the friction members are more homogeneous compared to other geometric shapes. The

distance from the center of each friction member to the center of the apparatus (x_F) is approximately 97.5 mm. Moreover, there are four elastomers (x_E=60 mm) with a diameter of 30 mm and eight elastomers (for four of them x_E=100 mm, for the others x_E=140 mm) with a diameter of 40 mm at each layer. The thickness of the friction members and elastomers at each layer is 10 mm. Thus, the shear rigidity (k_E) of the elastomer with 30 mm is calculated as 51.11 kN/m, with 40 mm as 90.85 kN/m. Using Eq. 1, the moment capacity of the friction members is obtained $M_F=8\cdot0.4\cdot0.0975.T_F=0.312T_F$ kNm. It was assumed that the connections are analyzed until the end of the story drift of 7% radian. Therefore using Eq. 2, the moment capacity of the elastomers is obtained $M_E=8\cdot(4\cdot51.11\cdot0.07\cdot0.06^2+4\cdot90.85\cdot0.07\cdot0.1^2+4\cdot90.85\cdot0.07\cdot0.14^2)=6.44$ kNm. In this case, the moment to be carried by the friction members is obtained as M_F = 255.01 kNm, and the total pretension to be applied to the bolts is obtained as T_F = 817.34 ≈ 818 kN. The total required pretension force is distributed in such a way that twice as much is applied to the main bolt as to the additional bolts. Thus, 274 kN of pretension force was applied to the main bolt and 136 kN to each additional bolt.

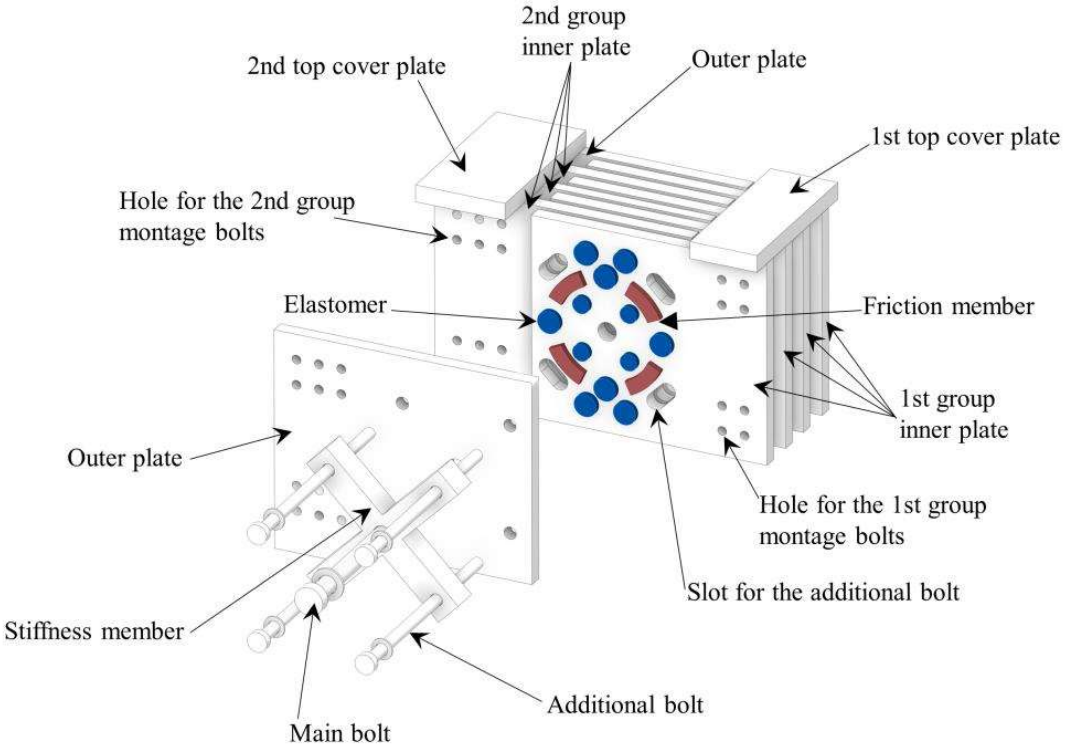


Fig. 6. The exploded 3D view of the apparatus

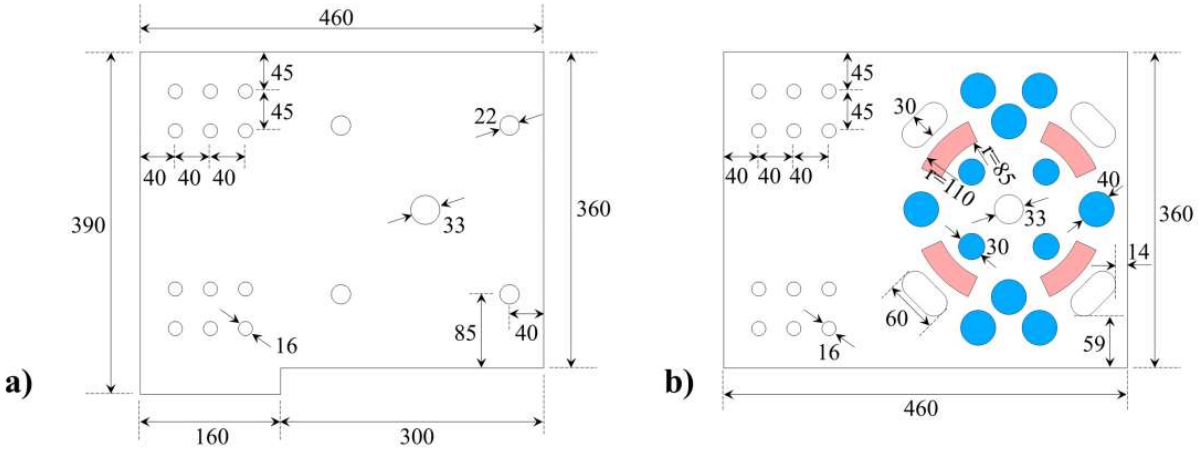
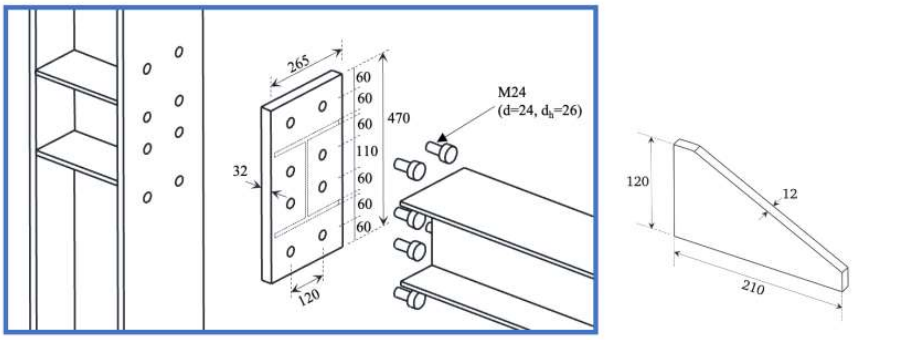


Fig. 7. The dimensions of outer and inner plates and friction members

The four-bolt end-plate connections (4E and 4ES) were designed according to ANSI/AISC 358-16. The design procedure of the connections can be seen in (Yılmaz, 2022). The dimensions of the 4E and 4ES connections are given in Fig. 8.



a) Connection zone of 4E and 4ES **b)** End-plate stiffener of 4ES

Fig. 8. The dimensions of 4E and 4ES connections

All components of all connections were modeled with SOLID186, which is a higher-order twenty-node three-dimensional hexahedral solid element with three degrees of freedom per node for finite element modeling. An elaborate mesh was adopted to obtain more sensitive results. FESA connection has 421248 nodes and 71772 elements, while 4E and 4ES connections have 221383 and 235886 nodes and 42398 and 45044 elements, respectively. Detailed information about the mesh structures of the connections can be seen in (Yılmaz, 2022). Moreover, each connecting component of the finite element model has surface-to-surface contact elements (CONTA174) or node-to-node contact elements (CONTA178). CONTA174 was used to model frictional contact (able to separate and slide) with a non-linear nature, while CONTA178 was used to model bonded contact with a linear nature.

3.2. Results and discussion

A comparison of the moment-rotation hysteretic curves between the FESA connection and bolted end-plate connections is given in Fig. 9. As can be seen in Fig. 9, the moment-rotation curve of the FESA connection shows a very stable behavior with no moment strength reduction. The moment value that the apparatus reaches at 7% radian rotation at the end of the analysis is 254.7 kNm, which is very close to M_{app}=261.4 kNm. In the 4E connection, a decrease in moment strength occurs after 6% radian rotation value, while in the 4ES connection, a decrease in moment strength occurs after 4% radian rotation value. Also, the moment values at 4% radian rotation for all connections are more than $0.80M_p$. Therefore, the required performance according to AISC 341-16 (AISC, 2016) is achieved for beam-to-column connections to be used in special moment frames in earthquake zones.

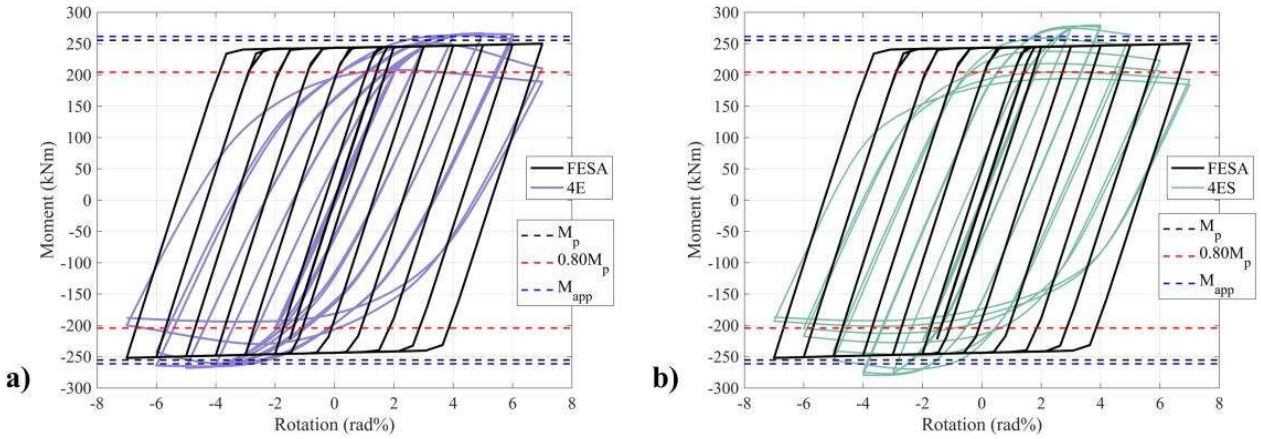


Fig. 9. Comparison of the moment-rotation hysteretic curves: a) FESA vs. 4E, b) FESA vs. 4ES

The energy dissipation (E)-rotation curves and hysteretic equivalent viscous damping ratio (ξ_{hys})-rotation curves for all connections are given in Fig. 10. It is seen that the FESA connection dissipates more energy and has a viscous damping ratio compared to bolted end-plate connections. Compared to the 4E connection, the FESA connection dissipates 137.1% more energy at 4% rotation and 58.0% more energy at 7% rotation. Compared to the 4ES connection, the FESA connection dissipates 91.2% more energy at 4% rotation and 43.6% more energy at 7% rotation. A similar situation is observed when they are compared in terms of hysteretic viscous damping ratios. The FESA connection has 111.5% more viscous damping ratio at 4% rotation than the 4E connection, while it has 31.4% more viscous damping ratio at 7% rotation. Compared to the 4ES connection, the FESA connection has 68.5% more viscous damping ratio at 4% rotation and 14.1% more viscous damping ratio at 7% rotation. As seen here, the performance parameters of FESA connection are considerably higher than those of bolted end-plate connections.

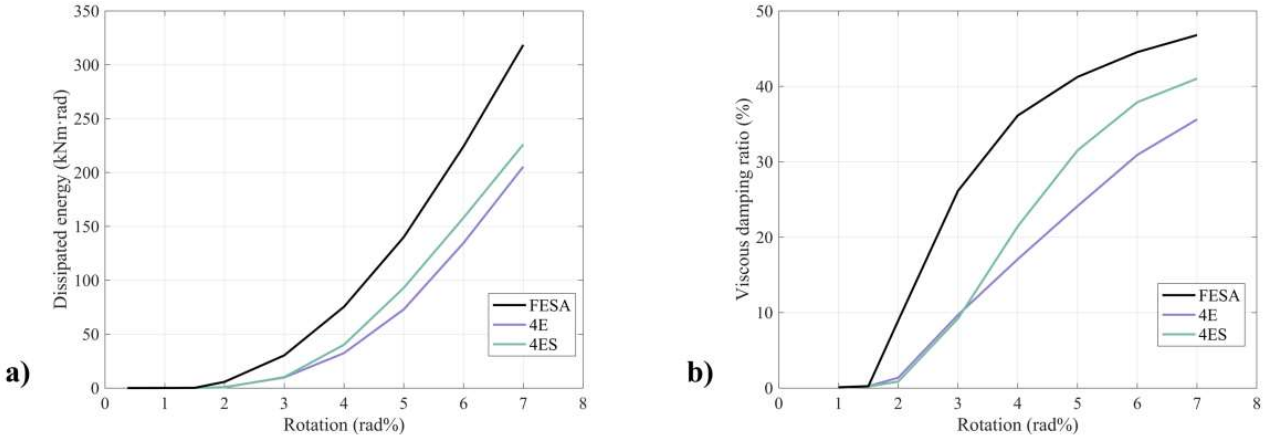


Fig. 10. a) Dissipated energy vs. rotation, b) Viscous damping ratio vs. rotation curves of the connections

Fig. 11 shows the equivalent plastic strain distributions for FESA and 4E connections to illustrate their failure modes. As seen here, plasticization does not occur in any structural members in the FESA connection, including the apparatus itself. However, as expected, plasticization occurs due to local buckling of the beam flanges and web in the bolted end-plate connections.

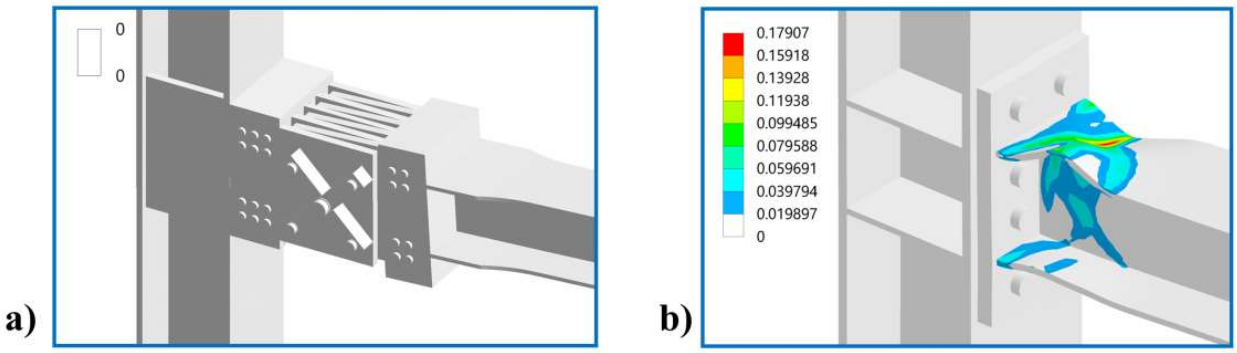


Fig. 11. Equivalent plastic strain distributions of the connections: a) FESA, b) 4E

As a result, for the parameters used in the study, the beam-to-column connection with the frictional and elastomeric seismic joint apparatus exhibited a better performance than the four bolted end-plate connections.

4. Conclusions

After the analyses and investigations, it was seen that beam-to-column connection with the proposed apparatus dissipates more energy and has an equivalent viscous damping ratio compared to the bolted end-plate connections presented in the codes such as TBER-2018 and AISC 358-16. Moreover, unlike the bolted end-plate connections, no plasticization was observed in any structural member of the beam-to-column connection with the proposed apparatus, including the apparatus itself. This ensures that the structure can be reused after a possible earthquake. In this study, the seismic joint apparatus developed by finite element simulation is able to compete with their foreign patented counterparts thanks to its ability to be modified as well as having the desired strength and flexibility of the moment connections prequalified in AISC 358-16.

Declaration of conflicting interests

The author(s) declared no potential conflicts of interest with respect to the research, authorship, and/or publication of this article.

Acknowledgments

The patent processes of the frictional and elastomeric seismic joint apparatus in Türkiye, EU, and USA are currently pending.

References

ANSI/AISC 341-16 (2016) Seismic Provisions for Structural Steel Buildings. American Institute of Steel Construction, Chicago.

ANSI/AISC 358-16 (2020) Prequalified Connections for Special and Intermediate Steel Moment Frames for Seismic Applications, including Supplements No. 1 and No. 2. American Institute of Steel Construction, Chicago.

Ansys® Academic Research Mechanical, Release 2020 R2. ANSYS, Inc.

Calado L, Proença JM, Espinha M, Castiglioni CA (2013) Hysteretic behaviour of dissipative bolted fuses for earthquake resistant steel frames. Journal of Constructional Steel Research 85:151–162.

Francavilla AB, Latour M, Piluso V, Rizzano G (2020) Design criteria for beam-to-column connections equipped with friction devices. Journal of Constructional Steel Research 172:106240.

Garoosi ARM, Tahamouli Roudsari M, Hashemi BH (2018) Experimental evaluation of rigid connection with reduced section and replaceable fuse. Structures 16:390–404.

Gerami M, Saberi H, Saberi V, Daryan AS (2011) Cyclic behavior of bolted connections with different arrangement of bolts. Journal of Constructional Steel Research 67:690–705.

Jiang ZQ, Yang XF, Dou C, Li C, Zhang AL (2019) Cyclic testing of replaceable damper: Earthquake-resilient prefabricated column-flange beam-column joint. Engineering Structures 183:922–936.

Molavi R, Izadinia M, Shahidi AR (2020) Numerical and experimental studies on cyclic behavior of beam-to-column connection with yielding steel damper. International Journal of Steel Structures 20:480–492.

Oh SH, Kim YJ, Ryu HS (2009) Seismic performance of steel structures with slit dampers. Engineering Structures 31:1997–2008.

Peng H, Ou J, Mahin S (2020) Design and numerical analysis of a damage-controllable mechanical hinge beam-to-column connection. Soil Dynamics and Earthquake Engineering 133:106149.

Richards PW, Oh SS (2019) Cyclic behavior of replaceable shear fuse connections for steel moment frames. Journal of Structural Engineering 145:04019156.

Sadeghi SN, Heidarpour A, Zhao XL, Al-Mahaidi R (2017) An innovative I-beam to hybrid fabricated column connection: Experimental investigation. Engineering Structures 148:907–923.

Saravanan M, Goswami R, Palani GS (2021) Energy dissipative beam-column connection for earthquake resistant moment frames. Journal of Constructional Steel Research 176:106428.

Sarkisian M, Mathias N, Garai R, Uang CM, Kim DW (2011) Pin-fuse frame™: Full scale tests. SEAOC 2011 Convention Proceedings.

Shen Y, Christopoulos C, Mansour N, Tremblay R (2011) Seismic design and performance of steel moment-resisting frames with nonlinear replaceable links. Journal of Structural Engineering 137:1107–1117.

TBEC (2018) Türkiye Building Earthquake Code: Rules for Design of Buildings under Earthquake Effect. Ankara (in Turkish).

Tong L, Chen Y, Chen Y, Fang C (2016) Cyclic behaviour of beam-to-column joints with cast steel connectors. Journal of Constructional Steel Research 116:114–130.

Yan JB, Chen Y, Lin X (2020) Finite element analysis and parametric studies on hysteretic behaviours of high strength steel T-joints with damage-control fuses. Thin-Walled Structures 148:106574.

Yılmaz O (2022) Development of Damaged or Non-damaged High Energy Dissipative Moment Connections in Seismic Resistant Steel Frames. PhD Dissertation, Yildiz Technical University (in Turkish).

Yılmaz O, Bekiroğlu S (2021) Development of a frictional and elastomeric seismic joint apparatus for use in buildings. In:14th International Congress on Advances in Civil Engineering (ACE2020-21), pp. 260-267.